Solvent-Induced Negative Energetic Elasticity in a Lattice Polymer Chain

Nobu C. Shirai[1,*,†] and Naoyuki Sakumichi[2,*,‡]
[1]*Center for Information Technologies and Networks, Mie University, Tsu, Mie 514-8507, Japan*
[2]*Department of Chemistry and Biotechnology, Graduate School of Engineering, The University of Tokyo,*
7-3-1 Hongo, Bunkyo-ku, Tokyo 113-8656, Japan

(Received 15 February 2022; revised 8 August 2022; accepted 1 March 2023; published 4 April 2023)

The negative internal energetic contribution to the elastic modulus (negative energetic elasticity) has been recently observed in polymer gels. This finding challenges the conventional notion that the elastic moduli of rubberlike materials are determined mainly by entropic elasticity. However, the microscopic origin of negative energetic elasticity has not yet been clarified. Here, we consider the n-step interacting self-avoiding walk on a cubic lattice as a model of a single polymer chain (a subchain of a network in a polymer gel) in a solvent. We theoretically demonstrate the emergence of negative energetic elasticity based on an exact enumeration up to $n = 20$ and analytic expressions for arbitrary n in special cases. Furthermore, we demonstrate that the negative energetic elasticity of this model originates from the attractive polymer–solvent interaction, which locally stiffens the chain and conversely softens the stiffness of the entire chain. This model qualitatively reproduces the temperature dependence of negative energetic elasticity observed in the polymer-gel experiments, indicating that the analysis of a single chain can explain the properties of negative energetic elasticity in polymer gels.

DOI: 10.1103/PhysRevLett.130.148101

Since the widespread acceptance of the macromolecular hypothesis [1], the entropic elasticity originating from flexible polymer chains in rubberlike materials has been investigated experimentally and theoretically [2–4]. The simplest theoretical explanations for entropic elasticity are provided by statistical models of ideal chains. For example, the random walk, freely jointed chain, and freely rotating chain models are described in textbooks on statistical mechanics [5,6], polymer physics [7,8], and soft matter physics [9].

Rubberlike materials composed of polymer chains exhibit an interplay between entropic (G_S) and energetic (G_U) contributions to the elastic modulus ($G = G_S + G_U$). In the case of conventional natural and synthetic rubbers, $|G_U|$ is significantly smaller than G_S [2–4]. A small $|G_U|$ is considered to originate from the conformational change of polymer chains, which has been theoretically modeled such as the rotational isometric state model [10]. By contrast, the significant negative G_U was recently observed in a chemically crosslinked polymer gel, i.e., a polymer network containing a large amount of solvent [11–13]. In this observation, $|G_U|$ is significantly larger than that of the energetic elasticity originating from conformational changes, and $|G_U|$ reaches the same order of magnitude as G, as shown in Fig. 1(a).

Although two previous studies [11,13] measured the shear modulus G over a narrow temperature (T) range where G can be approximated as a linear function of T, the

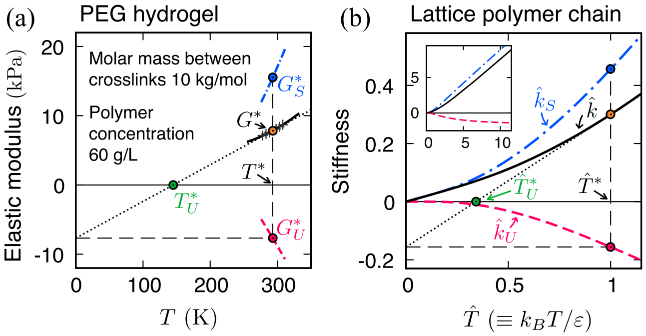

FIG. 1. Experimental results for a polymer gel [11,13] and theoretical results of the lattice polymer chain model. (a) Temperature dependence of shear modulus G of poly(ethylene glycol) (PEG) hydrogel for $T = 278$–308 K, including the midpoint $T^* = 293$ K [seven points, including the orange point (G^*) in the center]. These data are obtained from Refs. [11,13]. The black solid curve is the fitted quadratic function of these points. The dotted line is the tangent of the solid curve at the reference temperature T^*, which intersects with the horizontal axis at T^*_U (> 0) and the vertical axis at G^*_U (< 0). Temperature dependencies of G_U (pink dashed curve) and G_S (blue dot-dashed curve) are calculated from the fitted quadratic function. (b) Temperature dependence of stiffness ($\hat{k}$) of lattice polymer chain model for $(n, r) = (20, 10a)$ and its energetic ($\hat{k}_U$) and entropic ($\hat{k}_S$) contributions. The tangent (dotted line) of $\hat{k}$ at $\hat{T}^*$ intersects with the horizontal axis at $\hat{T}^*_U$ (> 0) and vertical axis at $\hat{k}^*_U \equiv \hat{k}_U(r, \hat{T}^*)$ (< 0).

---

combination of both results shows that G is an increasing convex function of T, as shown in Fig. 1(a). Here, T dependence of G is fitted by quadratic function (black solid curve), and the tangent of the fitted curve (dotted line) at the reference temperature $T^* = 293$ K intersects with the horizontal axis at T_U^* and vertical axis at G_U^*. These two experiments had the same conditions, excluding the temperature ranges; Ref. [11] used $T = 278$–298 K, whereas Ref. [13] used $T = 288$–308 K. By shifting T^* from 288 (Ref. [11]) to 298 K (Ref. [13]), the values of T_U^* increased. These results imply that (i) G is an increasing convex function of T, (ii) T_U^* depends on the reference temperature T^*, and (iii) G_U is a monotonically decreasing function of T.

In this Letter, focusing on a subchain (i.e., a chain between adjacent crosslinks) in the polymer network of polymer gels, we theoretically demonstrate the emergence of negative energetic elasticity in a single polymer chain model on a lattice. Notably, the previous experimental studies [11,13] show that G is described as $G = a(T - T_U^*)$ in a narrow temperature range, where a depends on the polymer network topology, but T_U^* does not [see Eqs. (7) and (9) in Ref. [12]]. Thus, network topology does not contribute to the proportion of energetic elasticity to entropic elasticity ($G_U^*/G_S^* = -T_U^*/T^*$), suggesting that a subchain is sufficient to investigate G_U^*/G_S^*. As shown in Figs. 1(a) and 1(b), this polymer chain model explains G_U as a monotonically decreasing function of temperature in polymer gel experiments. Furthermore, we provide a microscopic mechanism for the emergence of negative energetic elasticity by examining the polymer–solvent interaction strength in this model.

Lattice polymer chain model.—We consider a single polymer chain model surrounded by solvent molecules on a simple cubic lattice (three dimensions). This model was first introduced by Orr for highly dilute polymer solutions [14] and is one of the simplest ways to express the interaction between a polymer chain and solvent molecules. In Figs. 2(a) and 2(b), we use a square lattice (two dimensions) for illustration. As indicated in Fig. 2(a), this model consists of solvent molecules and a polymer chain represented by an n-step self-avoiding walk (SAW) [15], which has n bonds connecting $n+1$ consecutive and distinct lattice sites (i.e., the polymer segments). The energy function of the model is given by

$$E(\omega) = \varepsilon_{\mathrm{pp}} m_{\mathrm{pp}}(\omega) + \varepsilon_{\mathrm{ps}} m_{\mathrm{ps}}(\omega) + \varepsilon_{\mathrm{ss}} m_{\mathrm{ss}}(\omega), \qquad (1)$$

where ω denotes the configuration of SAWs, and $m_{\mathrm{pp}}(\omega)$, $m_{\mathrm{ps}}(\omega)$, and $m_{\mathrm{ss}}(\omega)$ are the numbers of the polymer–polymer, polymer–solvent, and solvent–solvent contact pairs, respectively. Here, the interaction energies acting between each pair are $\varepsilon_{\mathrm{pp}}$, $\varepsilon_{\mathrm{ps}}$, and $\varepsilon_{\mathrm{ss}}$, respectively. In Eq. (1), we do not consider the bending energetic terms, which are essential for semiflexible polymers [16], to focus on the solvent-induced energetic elasticity.

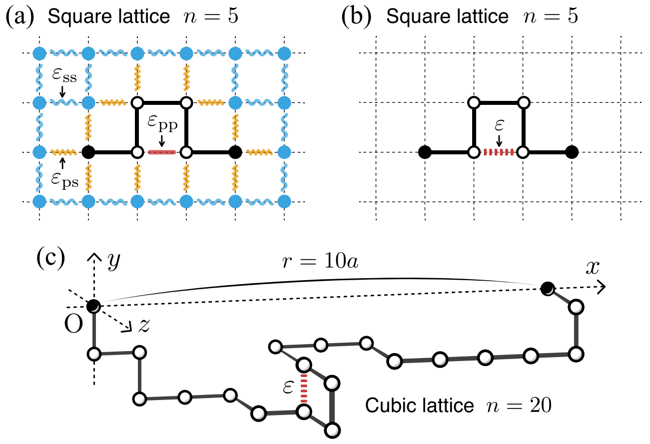

FIG. 2. (a) Two-component model of single polymer chain (open and filled black circles connected with lines) and solvent molecules (light-blue filled circles) on square lattice. There are three types of nearest-neighbor interactions. (b) Reduced model mathematically equivalent to (a). (c) Example of interacting self-avoiding walk on cubic lattice with on-axis constraint on end-to-end vector.

Once the entire lattice size is given, the total number of contact pairs, $m_{\mathrm{pp}}(\omega) + m_{\mathrm{ps}}(\omega) + m_{\mathrm{ss}}(\omega)$, is constant. In addition, we can derive $2m_{\mathrm{pp}}(\omega) + m_{\mathrm{ps}}(\omega) = (z-2)n + z$ by counting solvent molecules surrounding ω. Here, z is the coordination number of a lattice, e.g., $z = 4$ and 6 for the square and cubic lattices, respectively. Thus, when n is constant, Eq. (1) is rewritten [9,14] as

$$E(\omega) = \varepsilon m(\omega), \qquad (2)$$

where a constant term has been omitted, and $\varepsilon \equiv \varepsilon_{\mathrm{pp}} - 2\varepsilon_{\mathrm{ps}} + \varepsilon_{\mathrm{ss}}$ and $m(\omega) \equiv m_{\mathrm{pp}}(\omega)$. Here, the original model illustrated in Fig. 2(a) was reduced to the so-called interacting SAW [17] shown in Fig. 2(b), which is a single-chain system with the intrachain interaction. The interacting SAW reduces to the (noninteracting) SAW at $\varepsilon = 0$. Notably, many studies on the interacting SAW have focused on the self-attractive condition ($\varepsilon < 0$) to investigate the collapse transition [18–22]. By contrast, this study focuses mainly on the self-repulsive condition ($\varepsilon > 0$) to investigate the effect of attractive polymer–solvent interactions.

Energetic and entropic elasticities in lattice polymer chain.—To calculate the stiffness (a single-chain counterpart of the elastic modulus) of the lattice polymer chain model, we impose an on-axis constraint on the end-to-end vector of ω. Here, the length of the vector is r, and the direction of the vector is the same as the x axis, as shown in Fig. 2(c). The partition function with the on-axis constraint using Eq. (2) is given by

$$Z(r,T) = \sum_{m=0}^{m_{\mathrm{ub}}} W_{n,m}(r) e^{-\varepsilon m/(k_B T)}, \qquad (3)$$

where k_B is the Boltzmann constant, T is the absolute temperature, and $W_{n,m}(r)$ is the number of possible ω for a given set of n, r, and m. In Eq. (3), $m_{\rm ub}$ is an upper bound of m summation [i.e., $W_{n,m}(r) = 0$ for $m \geq m_{\rm ub} + 1$], which is discussed in Supplemental Material, Sec. S1 [23]. The corresponding free energy is $A(r, T) = -k_B T \ln Z(r, T)$.

We define the stiffness of the lattice polymer chain model with the on-axis constraint. In the continuum limit ($n \to \infty$ and lattice spacing $a \to 0$), the stiffness is defined as the second derivative of the free energy:

$$k(r,T) \equiv \frac{\partial^2 A(r,T)}{\partial r^2} = k_B T \left[\left(\frac{\frac{\partial Z(r,T)}{\partial r}}{Z(r,T)} \right)^2 - \frac{\frac{\partial^2 Z(r,T)}{\partial r^2}}{Z(r,T)} \right]. \quad (4)$$

Thus, we define the finite difference form of stiffness as

$$k(r,T) \equiv k_B T \left[\left(\frac{1}{Z(r,T)} \sum_{m=0}^{m_{\rm ub}} \frac{\Delta W_{n,m}(r)}{\Delta r} e^{-\varepsilon m/(k_B T)} \right)^2 - \frac{1}{Z(r,T)} \sum_{m=0}^{m_{\rm ub}} \frac{\Delta^2 W_{n,m}(r)}{\Delta r^2} e^{-\varepsilon m/(k_B T)} \right], \quad (5)$$

where the first- and second-order differences of $W_{n,m}(r)$ are given by $\Delta W_{n,m}(r) \equiv [W_{n,m}(r+\Delta r) - W_{n,m}(r-\Delta r)]/2$, and $\Delta^2 W_{n,m}(r) \equiv W_{n,m}(r+\Delta r) - 2W_{n,m}(r) + W_{n,m}(r-\Delta r)$, respectively. Here, $\Delta r \equiv 2a$ because ω exists only for odd $\hat{r} \equiv r/a$ for odd n and only for even $\hat{r}$ for even n (see Supplemental Material, Sec. S11 [23]).

We decompose the elasticity into its energetic and entropic contributions as $k = k_U + k_S$ in the same way as in Refs. [11,12]. According to thermodynamics, $A = U - TS$, where U is the internal energy and S is the entropy. Thus, in the continuum limit, the energetic and entropic contributions are $k_U(r,T) \equiv \partial^2 U(r,T)/\partial r^2$ and $k_S(r,T) \equiv -T\partial^2 S(r)/\partial r^2$, respectively. From Maxwell's relation, we have $k_S(r,T) = T\partial k(r,T)/\partial T$. Thus, we calculate $k_S(r,T) = T\partial k(r,T)/\partial T$ and $k_U = k - k_S$ in the lattice polymer chain model using Eq. (5).

Exact enumeration and derivation of polynomial functions.—We exactly enumerate $W_{n,m}(r)$ for $1 \leq n \leq 20$ using the simplest recursive algorithm [27] with two pruning algorithms, considering the octahedral symmetry of the simple cubic lattice and the reachability of ω to a specific endpoint (see Supplemental Material, Sec. S2 [23]). The complete lists of $W_{n,m}(r)$ are provided in Sec. S11 of Supplemental Material [23]. Those lists are consistent with the results reported in Refs. [14,28–37] (see Supplemental Material, Sec. S3 [23]). Using the lists of $W_{n,m}(r)$ with additional results up to $n = 26$ for $r = (n-8)a$, we exactly derive the polynomial functions $W_{n,m}((n-2)a)$, $W_{n,m}((n-4)a)$, $W_{n,m}((n-6)a)$, and $W_{n,m}((n-8)a)$ for arbitrary integers n and m, which are provided in Sec. S12 of Supplemental Material [23].

Emergence of negative energetic elasticity.—From the lists of $W_{n,m}(r)$, we can analytically calculate k, k_U, and k_S. Figure 1(b) shows a representative result for $\varepsilon > 0$ and $(n, r) = (20, 10a)$. Here, we introduce the dimensionless quantities $\hat{k} \equiv a^2 k/\varepsilon$, $\hat{k}_U \equiv a^2 k_U/\varepsilon$, $\hat{k}_S \equiv a^2 k_S/\varepsilon$, and $\hat{T} \equiv k_B T/\varepsilon$. Figure 1(b) demonstrates the emergence of the solvent-induced negative energetic elasticity ($k_U < 0$) in the model. Figure 2(c) displays an example of ω for $r = 10a$. In this Letter, we use $r = 10a$ for the illustration [e.g., Fig. 1(b)] because the maximum value of $|k_U|/k$ is larger than $r \neq 10a$. Although the extent of k_U/k depends on r, the negative k_U can be observed for different $n \geq 6$ and r. Notably, we find that $k_U < 0$ for arbitrary $n \geq 13$, $\varepsilon > 0$, and positive finite T using the polynomial functions $W_{n,m}((n-2)a)$, $W_{n,m}((n-4)a)$, $W_{n,m}((n-6)a)$, and $W_{n,m}((n-8)a)$ (see Supplemental Material, Sec. S13 [23]).

Figures 1(a) and 1(b) demonstrate the qualitative consistency between the previous experimental results for the shear modulus G of the poly(ethylene glycol) (PEG) hydrogel [11,13] and our results. These results suggest that negative energetic elasticity ($G_U < 0$) in the polymer gel originates from a single chain ($k_U < 0$).

To examine the effect of the sign of ε on the energetic elasticity, we show the dependence of the stiffness $\hat{k}/\hat{T} = a^2 k/(k_B T)$ on $1/\hat{T} \equiv \varepsilon/(k_B T)$ in Fig. 3. [Note that $\hat{k} \to \infty$ and $\hat{k}_S \to \infty$ at $\varepsilon = 0$ (noninteracting SAW), whereas $0 < \hat{k}/\hat{T} < \infty$ and $0 < \hat{k}_S/\hat{T} < \infty$.] Figure 3 depicts that the energetic contributions are negative, zero, and positive for $\varepsilon > 0$, $\varepsilon = 0$, and $\varepsilon > 0$, respectively, for $(n, r) = (20, 10a)$.

As depicted in Fig. 1(b), $\hat{T}_U^* \equiv \hat{T}_U(\hat{T}^*)$ denotes the $\hat{T}$ intercept of the tangent of $\hat{k} = \hat{k}(\hat{T})$ at the reference temperature $\hat{T} = \hat{T}^*$. For polymer gels, T_U^* [Fig. 1(a)] is a key factor in the analysis of negative energetic elasticity because T_U^* does not depend on the polymer network topology [11,12]. In addition, in the lattice polymer chain

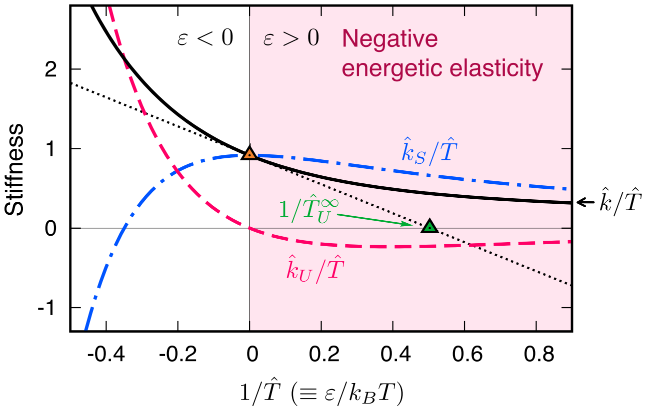

FIG. 3. Analytic curves of $\hat{k}/\hat{T}$, $\hat{k}_U/\hat{T}$, and $\hat{k}_S/\hat{T}$ as functions of $1/\hat{T}$ for $(n, r) = (20, 10a)$. The tangent (dotted line) of $\hat{k}/\hat{T}$ at $1/\hat{T}^* = 0$ intersects with the horizontal axis at $1/\hat{T}_U^\infty$. The condition for negative energetic elasticity ($\hat{k}_U/\hat{T} < 0$) is $\varepsilon > 0$.

model, T^*_U is a better measure of the negative energetic elasticity than k_U, because $T^*_U = \varepsilon \hat{T}^*_U / k_B$ is independent of the lattice spacing a, unlike $k_U = \varepsilon \hat{k}_U / a^2$, which depends on a.

We define $\hat{T}^\infty_U \equiv \lim_{\hat{T}^* \to \infty} \hat{T}_U(\hat{T}^*)$, which is a good indicator of the negative energetic elasticity in the sense that $\hat{T}^\infty_U > 0$ is identical to $\hat{k}_U < 0$ in the case of $\varepsilon > 0$. As shown in Fig. 3, the $1/\hat{T}$ intercept of the tangent of $\hat{k}/\hat{T}$ at $1/\hat{T} = 0$ corresponds to $1/\hat{T}^\infty_U$. Notably, $\hat{T}^\infty_U$ is a functional of $W_{n,m}(r)$ and is a rational number for a given set of n, r, and m (see Supplemental Material, Secs. S5, S6, and S7 [23]). In Fig. 4(a), we plot $\hat{T}^\infty_U$ that is calculated from $W_{n,m}(r)$ (the exact rational numbers of $\hat{T}^\infty_U$ are listed in Sec. S14 of Supplemental Material [23]).

We successfully determine the analytic expressions of $\hat{T}^\infty_U$ as the rational functions of n for $r = (n-2)a$, $(n-4)a$, and $(n-6)a$, using the polynomial functions of $W_{n,m}(r)$. For example,

$$\hat{T}^\infty_U(n,(n-2)a) = \frac{4(15n^8 - 356n^7 + 3766n^6 - 23016n^5 + 88019n^4 - 213804n^3 + 317784n^2 - 256008n + 81484)}{(n-1)(9n^8 - 204n^7 + 2026n^6 - 11648n^5 + 42733n^4 - 102444n^3 + 156272n^2 - 137656n + 53028)}. \tag{6}$$

The other rational functions, $\hat{T}^\infty_U(n,(n-4)a))$ and $\hat{T}^\infty_U(n,(n-6)a)$, are provided in Sec. S15 of Supplemental Material [23]. In Fig. 4(a), we overlay the three curves of these functions, which pass through all the corresponding points of $\hat{T}^\infty_U$.

Figure 4(b) shows $\hat{T}^\infty_U$ as a function of $(n-\hat{r})^\alpha/n$ for $\alpha = 3/4$. Here, the three curves of the analytic expressions and the points collapse onto a single master curve, except for the small values of n. A possible origin of the exponent $\alpha = 3/4$ is the reduction of the dimensionality from three to two by the on-axis constraint on the end-to-end vector, resulting in the universal critical exponent $\nu = 3/4$ of the two-dimensional SAW [38,39] (see Supplemental Material, Sec. S8 [23]).

Microscopic mechanism of negative energetic elasticity.—To characterize the microscopic properties of the lattice polymer chain model with a negative k_U, we evaluate the thermal average of the mean free path of the interacting SAW as

$$\ell(r,T) = \frac{1}{Z(r,T)} \sum_{m=0}^{m_{\mathrm{ub}}} \sum_{b=0}^{n-1} \frac{na}{b+1} W_{n,m,b}(r) e^{-\varepsilon m/(k_B T)}, \tag{7}$$

where b is the number of bending points of ω, and $W_{n,m,b}(r)$ is the number of ω for a given set of n, r, m, and b. In Eq. (7), $na/(b+1)$ is the mean free path for each ω (see Supplemental Material, Sec. S9 [23]). For example, $b = 4$ and 13 for ω in Figs. 2(b) and 2(c), respectively.

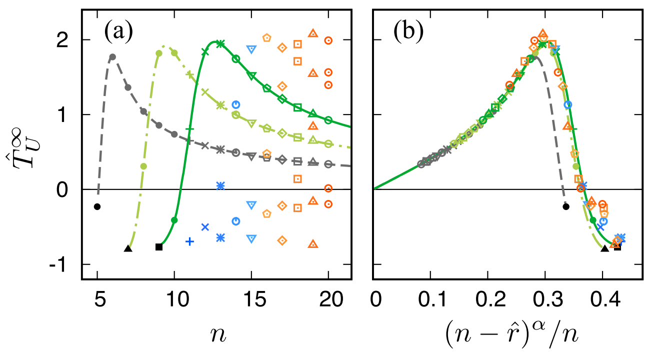

FIG. 4. (a) Exact values of $\hat{T}^\infty_U(n,r)$ for $n = 5, 6, \ldots, 20$ and three analytic curves for $r = (n-2)a$, $(n-4)a$, and $(n-6)a$, shown as gray dashed, light-green dot-dashed, and green solid curves, respectively. (b) Same points and curves plotted as functions of $(n-\hat{r})^\alpha/n$, where $\alpha = 3/4$. These collapse onto a single master curve.

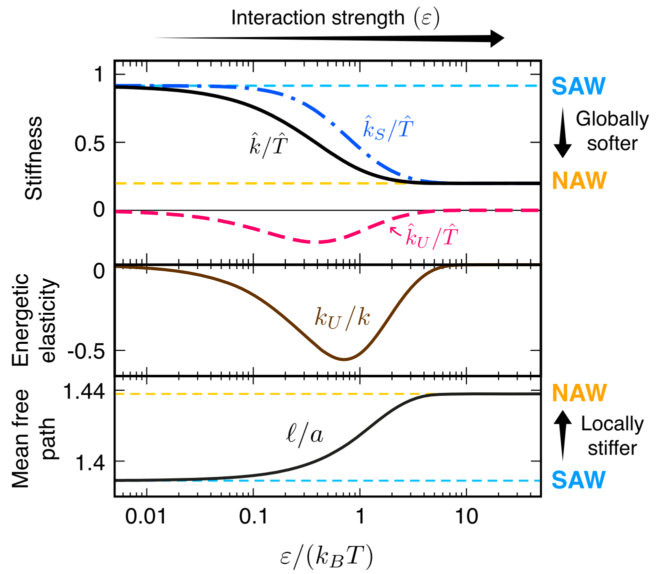

FIG. 5. Polymer–solvent interaction $[\varepsilon/(k_B T)]$ dependences of $\hat{k}/\hat{T}$, $\hat{k}_U/\hat{T}$, $\hat{k}_S/\hat{T}$ (top panel), k_U/k (middle panel), and ℓ/a (bottom panel) for $(n,r) = (20, 10a)$ and $\varepsilon > 0$. As ε increases, the lattice polymer chain model (i.e., interacting SAW) becomes globally softer and locally stiffer.

Figure 5 indicates that $\hat{k}/\hat{T} = a^2k/(k_BT)$ increases with $\varepsilon/(k_BT)$, whereas ℓ decreases with $\varepsilon/(k_BT)$. Here, $\hat{k}/\hat{T}$ characterizes the "global" stiffness of the whole polymer chain, whereas ℓ characterizes the "local" stiffness of the chain. Thus, the global and local stiffnesses are negatively correlated, which is also observed in various sets of (n, r) (see Supplemental Material, Sec. S4 [23]). These results confirm that polymer chains become locally stiffer because of the attractive interaction with solvent molecules, and globally softer because of the smaller curvature of free energy in the case of $\varepsilon > 0$ and $\hat{k}_U < 0$. This is the microscopic mechanism of negative energetic elasticity in the lattice polymer chain model.

Figure 5 also shows values corresponding to the SAW ($\varepsilon \to 0$) and neighbor-avoiding walk (NAW; $\varepsilon \to \infty$) [32,40,41] (see Supplemental Material, Sec. S10 [23]). The emergence of negative energetic elasticity is characterized by the crossover between the SAW and NAW, which only possess entropic elasticity. The minimum of k_U/k is -0.554 at $\varepsilon/(k_BT) \simeq 0.712$, where the interaction strength ε is the same order of magnitude as the thermal energy k_BT.

Concluding remarks.—We used the simplest lattice polymer chain model to explain both the energetic and entropic elasticities (Fig. 2). By exactly enumerating the configurations of this model, we obtained the stiffness of the chain and its energetic and entropic contributions (Fig. 3). This result demonstrates that the negative energetic elasticity originates from the polymer–solvent interaction. The three rational functions of T_U^∞ with respect to n are derived from the enumeration results (Fig. 4), revealing that negative energetic elasticity exists for all finite $n \geq 6$. We revealed a negative correlation between the stiffness of the whole polymer chain and the mean free path of the chain (Fig. 5). In short, locally stiffer chains are globally softer.

Although this simple model does not include chemical details, it qualitatively reproduces the temperature dependence of negative energetic elasticity observed in the experiments conducted on the PEG hydrogel [11,13] (Fig. 1). This fact indicates that negative energetic elasticity would emerge in various single polymer chains [42–44] and various polymer gels other than the PEG hydrogel. Therefore, this model provides a starting point for the further understanding of negative energetic elasticity in polymer chains and networks in solvents.

We thank Yuki Yoshikawa and Takamasa Sakai for allowing us to use the experimental data in Fig. 1(a) and for their useful comments, especially those regarding the temperature dependence of T_U^*. This study was supported by JSPS KAKENHI Grant No. JP22K13973 to N. C. S., and No. JP19K14672 and No. JP22H01187 to N. S.

---

[*] These authors contributed equally to this work.

[†] Corresponding author.
shirai@cc.mie-u.ac.jp

[‡] Corresponding author.
sakumichi@gel.t.u-tokyo.ac.jp

[1] H. Staudinger, Über polymerisation, Ber. Dtsch. Chem. Ges. **53**, 1073 (1920).

[2] K. H. Meyer and C. Ferri, Sur l'élasticité du caoutchouc, Helv. Chim. Acta **18**, 570 (1935).

[3] R. L. Anthony, R. H. Caston, and E. Guth, Equations of state for natural and synthetic rubber-like materials. I. Unaccelerated natural soft rubber, J. Phys. Chem. **46**, 826 (1942).

[4] J. E. Mark, Thermoelastic results on rubberlike networks and their bearing on the foundations of elasticity theory, J. Polym. Sci. **11**, 135 (1976).

[5] C. Kittel, *Thermal Physics* (Wiley, New York, 1969).

[6] H. B. Callen, *Thermodynamics and an Introduction to Thermostatistics* (Wiley, New York, 1991).

[7] P. G. de Gennes, *Scaling Concepts in Polymer Physics* (Cornell University Press, Ithaca, 1979).

[8] M. Rubinstein and R. H. Colby, *Polymer Physics* (Oxford University Press, Oxford, 2003).

[9] M. Doi, *Soft Matter Physics* (Oxford University Press, Oxford, 2013), 10.1093/acprof:oso/9780199652952.001.0001.

[10] P. J. Flory, *Statistical Mechanics of Chain Molecules* (Wiley Interscience, New York, 1969).

[11] Y. Yoshikawa, N. Sakumichi, U. Chung, and T. Sakai, Negative Energy Elasticity in a Rubberlike Gel, Phys. Rev. X **11**, 011045 (2021).

[12] N. Sakumichi, Y. Yoshikawa, and T. Sakai, Linear elasticity of polymer gels in terms of negative energy elasticity, Polym. J. **53**, 1293 (2021).

[13] T. Fujiyabu, T. Sakai, R. Kudo, Y. Yoshikawa, T. Katashima, U. Chung, and N. Sakumichi, Temperature Dependence of Polymer Network Diffusion, Phys. Rev. Lett. **127**, 237801 (2021).

[14] W. J. Orr, Statistical treatment of polymer solutions at infinite dilution, Trans. Faraday Soc. **43**, 12 (1947).

[15] N. Madras and G. Slade, *The Self-Avoiding Walk*, Probability and Its Applications (Birkhäuser, Boston, 1996), 10.1007/978-1-4612-4132-4.

[16] C. P. Broedersz and F. C. MacKintosh, Modeling semiflexible polymer networks, Rev. Mod. Phys. **86**, 995 (2014).

[17] C. Vanderzande, *Lattice Models of Polymers*, Cambridge Lecture Notes in Physics (Cambridge University Press, Cambridge, England, 1998), 10.1017/CBO9780511563935.

[18] D. C. Rapaport, On the polymer phase transition, Phys. Lett. **48A**, 339 (1974).

[19] D. Marenduzzo, A. Maritan, A. Rosa, and F. Seno, Stretching of a Polymer Below the θ Point, Phys. Rev. Lett. **90**, 088301 (2003).

[20] S. Kumar, I. Jensen, J. L. Jacobsen, and A. J. Guttmann, Role of Conformational Entropy in Force-Induced Biopolymer Unfolding, Phys. Rev. Lett. **98**, 128101 (2007).

[21] J. H. Lee, S. Y. Kim, and J. Lee, Exact partition function zeros of a polymer on a simple cubic lattice, Phys. Rev. E **86**, 011802 (2012).

[22] Y. H. Hsieh, C. N. Chen, and C. K. Hu, Efficient algorithm for computing exact partition functions of lattice polymer models, Comput. Phys. Commun. **209**, 27 (2016).

[23] See Supplemental Material at http://link.aps.org/supplemental/10.1103/PhysRevLett.130.148101 for (i) details of the enumeration method, (ii) derivations of analytic expressions, (iii) discussion on the data collapse shown in

Fig. 4(b), and (iv) complete lists of enumeration data, which includes Refs. [24–26].

[24] R. D. Schram, G. T. Barkema, and R. H. Bisseling, Exact enumeration of self-avoiding walks, J. Stat. Mech. (2011) P06019.

[25] R. D. Schram, G. T. Barkema, and R. H. Bisseling, SAWdoubler: A program for counting self-avoiding walks, Comput. Phys. Commun. **184**, 891 (2013).

[26] N. Clisby, R. Liang, and G. Slade, Self-avoiding walk enumeration via the lace expansion, J. Phys. A **40**, 10973 (2007).

[27] J. L. Martin, The exact enumeration of self-avoiding walks on a lattice, Math. Proc. Cambridge Philos. Soc. **58**, 92 (1962).

[28] M. E. Fisher and M. F. Sykes, Excluded-volume problem and the Ising model of ferromagnetism, Phys. Rev. **114**, 45 (1959).

[29] M. F. Sykes, Some counting theorems in the theory of the Ising model and the excluded volume problem, J. Math. Phys. (N.Y.) **2**, 52 (1961).

[30] M. F. Sykes, Self avoiding walks on the simple cubic lattice, J. Chem. Phys. **39**, 410 (1963).

[31] M. E. Fisher and B. J. Hiley, Configuration and free energy of a polymer molecule with solvent interaction, J. Chem. Phys. **34**, 1253 (1961).

[32] A. M. Nemirovsky, K. F. Freed, T. Ishinabe, and J. F. Douglas, Marriage of exact enumeration and $1/d$ expansion methods: Lattice model of dilute polymers, J. Stat. Phys. **67**, 1083 (1992).

[33] P. Butera and M. Comi, Critical specific heats of the N-vector spin models on the simple cubic and bcc lattices, Phys. Rev. B **60**, 6749 (1999).

[34] A. J. Guttmann, On the critical behaviour of self-avoiding walks, J. Phys. A **20**, 1839 (1987).

[35] C. Domb, J. Gillis, and G. Wilmers, On the shape and configuration of polymer molecules, Proc. Phys. Soc. London **85**, 625 (1965).

[36] N. J. A. Sloane, Entry A001412 in The On-Line Encyclopedia of Integer Sequences, https://oeis.org/A001412.

[37] J. Myers, Entry A174319 in The On-Line Encyclopedia of Integer Sequences, https://oeis.org/A174319.

[38] B. Nienhuis, Exact Critical Point and Critical Exponents of $\mathrm{O}(n)$ Models in Two Dimensions, Phys. Rev. Lett. **49**, 1062 (1982).

[39] B. Nienhuis, Critical behavior of two-dimensional spin models and charge asymmetry in the Coulomb gas, J. Stat. Phys. **34**, 731 (1984).

[40] G. Torrie and S. G. Whittington, Exact enumeration of neighbour-avoiding walks on the tetrahedral and body-centred cubic lattices, J. Phys. A **8**, 1178 (1975).

[41] T. Ishinabe and Y. Chikahisa, Exact enumerations of self-avoiding lattice walks with different nearest-neighbor contacts, J. Chem. Phys. **85**, 1009 (1986).

[42] K. Nakajima, H. Watabe, and T. Nishi, Single polymer chain rubber elasticity investigated by atomic force microscopy, Polymer **47**, 2505 (2006).

[43] A. Kolberg, C. Wenzel, K. Hackenstrass, R. Schwarzl, C. Rüttiger, T. Hugel, M. Gallei, R. R. Netz, and B. N. Balzer, Opposing temperature dependence of the stretching response of single PEG and PNiPAM polymers, J. Am. Chem. Soc. **141**, 11603 (2019).

[44] Y. Bao, Z. Luo, and S. Cui, Environment-dependent single-chain mechanics of synthetic polymers and biomacromolecules by atomic force microscopy-based single-molecule force spectroscopy and the implications for advanced polymer materials, Chem. Soc. Rev. **49**, 2799 (2020).